arXiv:1612.06482v1 [math-ph] 20 Dec 2016

THE BOUNDARY LENGTH AND POINT SPECTRUM ENUMERATION OF PARTIAL CHORD DIAGRAMS USING CUT AND JOIN RECURSION

JØRGEN ELLEGAARD ANDERSEN, HIROYUKI FUJI, ROBERT C. PENNER, AND CHRISTIAN M. REIDYS

Abstract. We introduce the boundary length and point spectrum, as a joint generalization of the boundary length spectrum and boundary point spectrum in [1]. We establish by cut-and-join methods that the number of partial chord diagrams filtered by the boundary length and point spectrum satisfies a recursion relation, which combined with an initial condition determines these numbers uniquely. This recursion relation is equivalent to a second order, non-linear, algebraic partial differential equation for the generating function of the numbers of partial chord diagrams filtered by the boundary length and point spectrum.

Contents

1. Introduction 1
2. Combinatorial proof of the cut-and-join equation 7
3. Non-oriented analogue of the cut-and-join equation 11
References 15

1. Introduction

A *partial chord diagram*, is a special kind of graph, which can be specified as follows. The graph consists of a number of line segments (which we will also call backbones) arranged along the real line (hence they come with an ordering) with a number of vertices on each. A number of semi-circles (called chords) arranged in the upper half plan are attached at a subset of the vertices of the line segments, in such a way that no two chords have endpoints on the line segments in common. The vertices which are not attached to chord ends are called the marked points. A *chord diagram* is by definition a partial chord diagram with no marked points. Partial chord diagrams occur in many branches of mathematics, including topology [12, 15], geometry [8, 9, 2] and representation theory [13]. Furthermore, they play a very prominent role in macro molecular biology. Please see the introduction of [6] for a short review of these applications.

Acknowledgments: The authors thank Masahide Manabe and Piotr Sułkowski for useful comments. JEA and RCP are supported by the Centre for Quantum Geometry of Moduli Spaces which is funded by the Danish National Research Foundation. The research of HF is supported by the Grant-in-Aid for Research Activity Start-up [# 15H06453], Grant-in-Aid for Scientific Research(C) [# 26400079], and Grant-in-Aid for Scientific Research(B) [# 16H03927] from the Japan Ministry of Education, Culture, Sports, Science and Technology.

As documented in [17, 25, 24, 11, 10, 7, 3, 4, 1, 23, 22, 5, 6], the notion of a *fatgraph* [18, 19, 20, 21] is a useful concept when studying partial chord diagrams[1]. A fatgraph is a graph together with a cyclic ordering on each collection of half-edges incident on a common vertex. A partial linear chord diagram c has a natural fatgraph structure induced from its presentation in the plane. The fatgraph c has canonically a two dimensional surface with boundary Σ_c associated to it (e.g. see Figure 1).

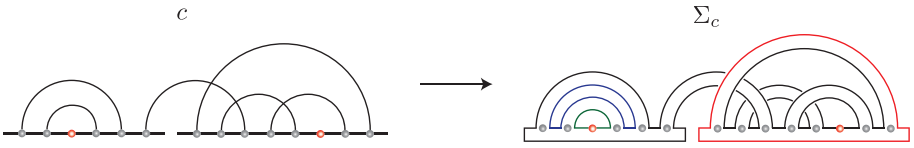

FIGURE 1. The partial chord diagram c and the surface Σ_c associated to the fatgraph with marked points. This partial chord diagram has the type $\{g,k,l;\{b_i\};\{n_i\};\{\ell_i\}\}=\{1,6,2;\{b_6=1,b_8=1\};\{n_0=2,n_1=2\};\{\ell_1=1,\ell_2=2,\ell_9=1\}\}$. The boundary length-point spectra are $\{m_{(1)}=1,m_{(0,0)}=2,m_{(0,0,0,0,0,1,0,0,0)}=1\}$.

We now recall the basic definitions from [1] for a partial chord diagram c.

- The number of chords, the number of marked points, and the number of backbones of c are denoted k, l, and b respectively.
- The Euler characteristic and the genus of Σ_c, are denoted χ and g respectively. If n is the number of boundary components of Σ_c, we have that
$$\chi = 2-2g, \tag{1}$$
and g obeys Euler's relation
$$2-2g = b-k+n. \tag{2}$$
- The *backbone spectrum* $\boldsymbol{b}=(b_0,b_1,b_2,\ldots)$ are assigned to c, if it has b_i backbones with precisely $i\geq 0$ vertices (of degree either two or three);
- The *boundary point spectrum* $\boldsymbol{n}=(n_0,n_1,\ldots)$ is assigned to c, if its boundary contains n_i connected components with i marked points;
- The *boundary length spectrum* $\boldsymbol{\ell}=(\ell_1,\ell_2,\ldots)$ is assigned to c, if the boundary cycles of the diagram consist of ℓ_K edge-paths of length $K\geq 1$, where the *length* of a boundary cycle is the number of chords it traverses counted with multiplicity (as usual on the graph obtained from the diagram by collapsing each backbone to a distinct point) *plus* the number of backbone undersides it traverses (or in other words, the number of traversed connected components obtained by removing all the chord endpoints from all the backbones).

[1] In [16, 14], the Schwinger-Dyson approach to the enumeration of chord diagrams is also discussed.

We now introduce the combination of the boundary length spectrum and the boundary point spectrum, namely our new boundary length and point spectrum.

- The *boundary length and point spectrum* $\boldsymbol{m} = (m_{(d_1,\dots,d_K)})$ is assigned to c, if its boundary contains $m_{(d_1,\dots,d_K)}$ connected components of length K with marked point spectrum $(d_1,\dots,d_K)$, meaning that there cyclically around the boundary components are d_1 marked points, then a chord or a backbone underside, then d_2 marked points, then a chord or a backbone underside, and so on all the way around the boundary component. In fact we will not need to distinguish which way around the boundary we go. Hence it is only the cyclic ordered tuple of the numbers $d_1,\dots,d_K$, which we need and which we denote as $\boldsymbol{d}_K = (d_1,\dots,d_K)$. We remark that some of the d_I $(1 \le I \le K)$ might be zero.

We have the following relations

$$\begin{aligned} b &= \sum_{i\ge 0} b_i,\ n = \sum_{i\ge 0} n_i = \sum_{K\ge 1} \ell_K = \sum_{K\ge 1}\sum_{\boldsymbol{d}_K} m_{\boldsymbol{d}_K}, \\ 2k+l &= \sum_{i>0} i b_i,\ l = \sum_{i>0} i n_i = \sum_{K\ge 1}\sum_{\boldsymbol{d}_K} |\boldsymbol{d}_K| m_{\boldsymbol{d}_K} \\ 2k+b &= \sum_{K\ge 1} K\ell_K = \sum_{K\ge 1}\sum_{\boldsymbol{d}_K} K m_{\boldsymbol{d}_K}, \end{aligned}$$

where $|\boldsymbol{d}_K| = \sum_{I=1}^{K} d_I$. For all K and i, we also have that

$$\ell_K = \sum_{\boldsymbol{d}_K} m_{\boldsymbol{d}_K}, \quad n_i = \sum_{K\ge 1}\sum_{i=|\boldsymbol{d}_K|} m_{\boldsymbol{d}_K}.$$

We define $\mathcal{M}_{g,k,l}(\boldsymbol{b},\boldsymbol{m})$ to be the number of connected partial chord diagrams of type $\{g,k,l;\boldsymbol{b};\boldsymbol{m}\}$ taken to be zero if there is none of the specified type. In [1], $\mathcal{N}_{g,k,l}(\boldsymbol{b},\boldsymbol{n},\boldsymbol{p})$ is defined as the number of distinct connected partial chord diagrams of type $\{g,k,l;\boldsymbol{b};\boldsymbol{n};\boldsymbol{p}\}$. We find the relation between these numbers by the following formula

$$\mathcal{N}_{g,k,l}(\boldsymbol{b},\boldsymbol{\ell},\boldsymbol{n}) = \sum_{\boldsymbol{m}\in M(\boldsymbol{\ell},\boldsymbol{n})} \mathcal{M}_{g,k,l}(\boldsymbol{b},\boldsymbol{m}),$$

where

$$M(\boldsymbol{\ell},\boldsymbol{n}) = \big\{\boldsymbol{m}\,\big|\,\ell_K = \sum_{\boldsymbol{d}_K} m_{\boldsymbol{d}_K},\ n_i = \sum_{K\ge 1}\sum_{i=|\boldsymbol{d}_K|} m_{\boldsymbol{d}_K}\big\}.$$

In particular, the numbers $\mathcal{N}_{g,k,l}(\boldsymbol{b},\boldsymbol{n})$ and $\mathcal{N}_{g,k,b}(\boldsymbol{\ell})$ are given by

$$\mathcal{N}_{g,k,l}(\boldsymbol{b},\boldsymbol{n}) = \sum_{\boldsymbol{\ell}} \mathcal{N}_{g,k,l}(\boldsymbol{b},\boldsymbol{\ell},\boldsymbol{n}), \quad \mathcal{N}_{g,k,b}(\boldsymbol{\ell}) = \sum_{\boldsymbol{n}}\sum_{\sum b_i = b} \mathcal{N}_{g,k,l=0}(\boldsymbol{b},\boldsymbol{\ell},\boldsymbol{n}),$$

For the index $\boldsymbol{b} = (b_i)$, we consider the variable $\boldsymbol{t} = (t_i)$ and denote

$$\boldsymbol{t}^{\boldsymbol{b}} = \prod_{i\ge 0} t_i^{b_i}.$$

And for the index $\boldsymbol{d} = (\boldsymbol{d}_K)$, we consider the variable $\boldsymbol{u} = (u_{\boldsymbol{d}_K})$ and denote

$$\boldsymbol{u}^{\boldsymbol{m}} = \prod_{K\ge 1}\prod_{\boldsymbol{d}_K} u_{\boldsymbol{d}_K}^{m_{\boldsymbol{d}_K}}$$

for any $\boldsymbol{m} = (\boldsymbol{m}_{\boldsymbol{d}_K})$. We define the orientable, multi-backbone, boundary length and point spectrum generating function $H(x,y;\boldsymbol{t};\boldsymbol{u}) = \sum_{b\geq 0}\mathcal{F}_b(x,y;\boldsymbol{t};\boldsymbol{u})$, where

$$H_b(x,y;\boldsymbol{t};\boldsymbol{u}) = \frac{1}{b!}\sum_{g=0}^{\infty}\sum_{k=2g+b-1}^{\infty}\sum_{\substack{\sum_K\sum_{\boldsymbol{d}_K} m_{\boldsymbol{d}_K}\\ =k-2g-b+2}}\sum_{\sum b_i=b}\mathcal{M}_{g,k,l}(\boldsymbol{b},\boldsymbol{m})x^{2g}y^k\boldsymbol{t}^{\boldsymbol{b}}\boldsymbol{u}^{\boldsymbol{m}}, \quad (3)$$

For an element $\boldsymbol{p} = (p_{(d_1,\ldots d_K)})$, where each $p_{(d_1,\ldots d_K)} \in \mathbb{Z}$, we write

$$\boldsymbol{p} = \boldsymbol{p}^+ - \boldsymbol{p}^-,$$

where $\boldsymbol{p}^+$ contains all the positive entries and $\boldsymbol{p}^-$ the absolute value of all the negative ones, which we assume to both be finite. We define the differential operator

$$D_{\boldsymbol{p}} = \prod_{\boldsymbol{d}} u_{\boldsymbol{d}}^{\boldsymbol{p}_{\boldsymbol{d}}^-}\prod_{\boldsymbol{d}}\left(\frac{\partial}{\partial u_{\boldsymbol{d}}}\right)^{\boldsymbol{p}_{\boldsymbol{d}}^+}.$$

We now define $s_{I,J,\ell,m}(\boldsymbol{d}_K)$, $s_{I,\ell,m}(\boldsymbol{d}_K)$ and $q_{I,J,\ell,m}(\boldsymbol{d}_K,\boldsymbol{f}_L)$ to be strings like $\boldsymbol{p}$ given by the following formulae

$$\begin{aligned}
&s_{I,J,\ell,m}(\boldsymbol{d}_K) = \boldsymbol{e}_{\boldsymbol{d}_K} - \boldsymbol{e}_{(d_1,\ldots,d_{I-1},d_I-\ell-1,m,d_{J+1},\ldots,d_K)} - \boldsymbol{e}_{(\ell,d_{I+1},\ldots,d_{J-1},d_J-m-1)},\\
&s_{I,\ell,m}(\boldsymbol{d}_K) = \boldsymbol{e}_{\boldsymbol{d}_K} - \boldsymbol{e}_{(d_1,\ldots,d_{I-1},\ell,m,d_{I+1},\ldots,d_K)} - \boldsymbol{e}_{(d_I-\ell-m-2)},\\
&q_{I,J,\ell,m}(\boldsymbol{d}_K,\boldsymbol{f}_L)\\
&= \boldsymbol{e}_{\boldsymbol{d}_K} + \boldsymbol{e}_{\boldsymbol{f}_L} - \boldsymbol{e}_{(d_1,\ldots,d_{I-1},d_I-\ell-1,m,f_{J+1},\ldots,f_L,f_1,\ldots,f_{J-1},f_J-m-1,\ell,d_{I+1},\ldots,d_K)}.
\end{aligned}$$

where $\boldsymbol{e}_{\boldsymbol{d}_K}$ denotes the sequence $(0,\ldots,0,1,0,\ldots)$ where the component 1 appears only at the entry indexed by $\boldsymbol{d}_K$. We further define the index $c_{I,J,\ell,h}(\boldsymbol{d}_K,\boldsymbol{f}_M)$ by the formula

$$\begin{aligned}
&c_{I,J,\ell,m}(\boldsymbol{d}_K,\boldsymbol{f}_L)\\
&= (d_1,\ldots,d_{I-1},d_I-\ell-1,m,f_{J+1},\ldots,f_L,f_1,\ldots,f_{J-1},f_J-m-1,\ell,d_{I+1},\ldots,d_K),
\end{aligned}$$

which is identical to the index on the last term of the above assignments.

Theorem 1.1 (Enumeration of partial chord diagrams filtered by their boundary length and point spectrum)**.**

Define the first and second order linear differential operators

$$M_0 = \sum_{K\geq 1}\sum_{\boldsymbol{d}_K}\left(\sum_{1\leq J<I\leq K}\sum_{\ell=0}^{d_I-1}\sum_{m=0}^{d_J-1}D_{s_{I,J,\ell,m}(\boldsymbol{d}_K)} + \sum_{I=1}^{K}\sum_{\ell,m=0}^{d_I-1}D_{s_{I,\ell,m}(\boldsymbol{d}_K)}\right), \quad (4)$$

$$M_2 = \frac{1}{2}\sum_{K,L\geq 1}\sum_{\boldsymbol{d}_K,\boldsymbol{f}_L}\sum_{I=1}^{K}\sum_{J=1}^{L}\sum_{\ell=0}^{d_I-1}\sum_{m=0}^{d_J-1}D_{q_{I,J,\ell,h}(\boldsymbol{d}_K)}, \quad (5)$$

and the quadratic differential operator

$$S(H) = \frac{1}{2}\sum_{K,L\geq 1}\sum_{\boldsymbol{d}_K,\boldsymbol{f}_L}\sum_{I=1}^{K}\sum_{J=1}^{L}\sum_{\ell=0}^{d_I-1}\sum_{m=0}^{f_L-1}u_{c_{I,J,\ell,m}(\boldsymbol{d}_K,\boldsymbol{f}_L)}D_{\boldsymbol{d}_K}(H)D_{\boldsymbol{f}_L}(H)\,. \quad (6)$$

Then the following partial differential equations hold

$$\frac{\partial H_1}{\partial y} = (M_0 + x^2M_2)H_1, \quad \frac{\partial H}{\partial y} = (M_0 + x^2M_2 + S)H. \quad (7)$$

Together with the initial conditions

$$H_1(x, y = 0; \boldsymbol{t} = (t_1); \boldsymbol{u}) = u_{(0)} t_1, \quad H(x, y = 0; \boldsymbol{t}; \boldsymbol{u}) = \sum_{i \geq 1} u_{(i)} t_i, \tag{8}$$

they determine the functions H_1 and H uniquely.

In this article, we also consider the non-oriented analogue of partial chord diagrams. The generalization of the above analysis is straightforward, as we will now explain. A *non-oriented* partial chord diagrams, is a partial chord diagram together with a decoration of a binary variable at each chord, which indicates if the chord is *twisted* or not. When associating the surface Σ_c, to a non-oriented partial chord diagram, a twisted band is associated along twisted chords as indicated in Figure 2. By this construction, 2^k orientable and non-orientable surfaces are obtained from one partial chord diagram with k chords, when we vary over all assignments of twisting or not to the k chords. In the non-oriented case, we have the following definition of the Euler characteristic.

- Euler characteristic χ.
  The Euler characteristic of the two dimensional surface Σ_c is defined by the formula

$$\chi = 2 - h, \tag{9}$$

  where h is the number of cross-caps and we have Euler's relation

$$2 - h = b - k + n. \tag{10}$$

With this set-up, the enumeration of the non-oriented partial chord diagrams is considered in parallel to the oriented case discussed above with a small change for the boundary length and point spectrum $\boldsymbol{m}$. In this non-oriented case, there are now induced orientation on the boundaries of Σ_c and hence for an index $\boldsymbol{d}_K = (d_1, \ldots, d_K)$ corresponding some boundary component of Σ_c, we not only need to consider this tuple up to cyclic permutation of the tuple, but also reversal of the order

$$\boldsymbol{d}_K = (d_1, d_2, \ldots, d_K) = (d_K, \ldots d_2, d_1).$$

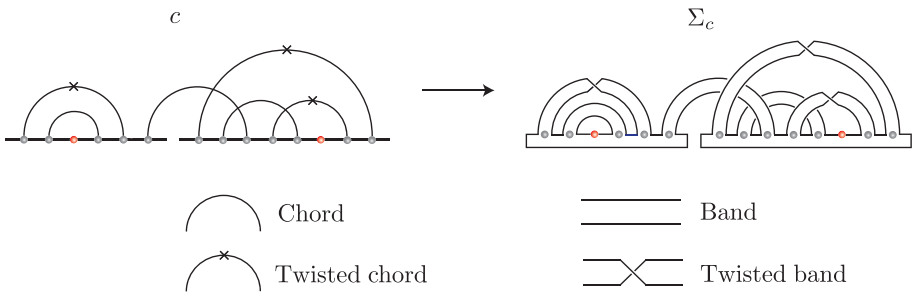

FIGURE 2. The non-oriented surface constructed out of untwisted and twisted chords.

Let $\widetilde{\mathcal{M}}_{h,k,l}(\boldsymbol{b}, \boldsymbol{m})$ be the number of non-oriented partial chord diagrams of type $\{h, k, l; \boldsymbol{b}; \boldsymbol{m}\}$. In [1], $\widetilde{\mathcal{N}}_{h,k,l}(\boldsymbol{b}, \boldsymbol{\ell}, \boldsymbol{n})$ is defined as the number of non-oriented connected partial chord diagrams of type $\{h, k, l; \boldsymbol{b}; \boldsymbol{\ell}; \boldsymbol{n}\}$. These numbers are related

by the following formula

$$\widetilde{\mathcal{N}}_{h,k,l}(\boldsymbol{b},\boldsymbol{\ell},\boldsymbol{n}) = \sum_{\boldsymbol{m}\in M(\boldsymbol{\ell},\boldsymbol{n})} \widetilde{\mathcal{M}}_{h,k,l}(\boldsymbol{b},\boldsymbol{m}),$$

and the numbers $\widetilde{\mathcal{N}}_{h,k,l}(\boldsymbol{b},\boldsymbol{n})$ and $\widetilde{\mathcal{N}}_{h,k,b}(\boldsymbol{\ell})$ are given by

$$\widetilde{\mathcal{N}}_{h,k,l}(\boldsymbol{b},\boldsymbol{n}) = \sum_{\boldsymbol{\ell}} \widetilde{\mathcal{N}}_{h,k,l}(\boldsymbol{b},\boldsymbol{\ell},\boldsymbol{n}), \qquad \widetilde{\mathcal{N}}_{h,k,b}(\boldsymbol{\ell}) = \sum_{\boldsymbol{n}} \sum_{\sum b_i=b} \widetilde{\mathcal{N}}_{h,k,l=0}(\boldsymbol{b},\boldsymbol{\ell},\boldsymbol{n}).$$

We define the non-oriented generating function $\widetilde{H}(x,y;\boldsymbol{t};\boldsymbol{u}) = \sum_{b\geq 1}\widetilde{H}_b(x,y;\boldsymbol{t};\boldsymbol{u})$ to be given by

$$\widetilde{H}_b(x,y;\boldsymbol{t};\boldsymbol{u}) = \frac{1}{b!}\sum_{h=0}^{\infty}\sum_{k=h+b-1}^{\infty} \sum_{\substack{\sum_K \sum_{\boldsymbol{d}_K} m_{\boldsymbol{d}_K} \\ =k-h-b+2}} \sum_{\sum b_i=b} \widetilde{\mathcal{M}}_{h,k,l}(\boldsymbol{b},\boldsymbol{m}) x^h y^k \boldsymbol{t}^{\boldsymbol{b}}\boldsymbol{u}^{\boldsymbol{m}}. \quad (11)$$

We define $s^{\times}_{I,J,\ell,h}(\boldsymbol{d}_K)$, $s^{\times}_{I,\ell,h}(\boldsymbol{d}_K)$ and $q^{\times}_{I,J,\ell,h}(\boldsymbol{d}_K,\boldsymbol{f}_L)$ to be by

$$\begin{aligned}
&s^{\times}_{I,J,\ell,m}(\boldsymbol{d}_K) = \boldsymbol{e}_{\boldsymbol{d}_K} - \boldsymbol{e}_{(d_1,\ldots,d_{I-1},\ell,m,d_{J-1},\ldots,d_{I+1},d_J-\ell-1,d_J-m-1,d_{J+1},\ldots,d_K)},\\
&s^{\times}_{I,\ell,m}(\boldsymbol{d}_K) = \boldsymbol{e}_{\boldsymbol{d}_K} - \boldsymbol{e}_{(d_1,\ldots,d_{I-1},\ell,d_I-\ell-m-2,m,d_{I+1},\ldots,d_K)},\\
&q^{\times}_{I,J,\ell,m}(\boldsymbol{d}_K,\boldsymbol{f}_L)\\
&\quad = \boldsymbol{e}_{\boldsymbol{d}_K} + \boldsymbol{e}_{\boldsymbol{f}_M} - \boldsymbol{e}_{(f_1,\ldots,f_{J-1},f_J-m-1,\ell,d_{I-1},\ldots,d_1,d_K,\ldots,d_{I+1},d_I-\ell-1,m,f_{J+1},\ldots,f_L)}.
\end{aligned}$$

And we also define indices $c^{\times}_{I,J,\ell,h}(\boldsymbol{d}_K,\boldsymbol{f}_M)$ by the formula

$$\begin{aligned}
&c^{\times}_{I,J,\ell,h}(\boldsymbol{d}_K,\boldsymbol{f}_L)\\
&= (f_1,\ldots,f_{J-1},f_J-m-1,\ell,d_{I-1},\ldots,d_1,d_K,\ldots,d_{I+1},d_I-\ell-1,m,f_{J+1},\ldots,f_L),
\end{aligned}$$

which again, we note is identical to the index on the last term of the above assignments.

Theorem 1.2 (Enumeration of non-oriented partial chord diagrams filtered by their boundary length and point spectrum)**.**

Define the first and second order linear differential operators

$$M_1^{\times} = \sum_{K\geq 1}\sum_{\boldsymbol{d}_K}\left(\sum_{1\leq J<I\leq K}\sum_{\ell=0}^{d_I-1}\sum_{m=0}^{d_J-1} D_{s^{\times}_{I,J,\ell,m}(\boldsymbol{d}_K)} + \sum_{I=1}^{K}\sum_{\ell,m=0}^{d_I-1} D_{s^{\times}_{I,\ell,m}(\boldsymbol{d}_K)}\right), \quad (12)$$

$$M_2^{\times} = \frac{1}{2}\sum_{K,L\geq 1}\sum_{\boldsymbol{d}_K,\boldsymbol{f}_L}\sum_{I=1}^{K}\sum_{J=1}^{L}\sum_{\ell=0}^{d_I-1}\sum_{m=0}^{d_J-1} D_{q^{\times}_{I,J,\ell,m}(\boldsymbol{d}_K)}, \quad (13)$$

and the quadratic differential operator

$$S^{\times}(H) = \frac{1}{2}\sum_{K,L\geq 1}\sum_{\boldsymbol{d}_K,\boldsymbol{f}_L}\sum_{I=1}^{K}\sum_{J=1}^{L}\sum_{\ell=0}^{d_I-1}\sum_{m=0}^{f_L-1} u_{c^{\times}_{I,J,\ell,m}(\boldsymbol{d}_K,\boldsymbol{f}_L)} D_{\boldsymbol{d}_K}(H) D_{\boldsymbol{f}_L}(H)\,. \quad (14)$$

Then the following partial differential equations hold

$$\begin{aligned}
\frac{\partial \widetilde{H}_1}{\partial y} &= (M_0 + xM_1^{\times} + x^2(M_2+M_2^{\times}))\widetilde{H}_1,\\
\frac{\partial \widetilde{H}}{\partial y} &= (M_0 + xM_1^{\times} + x^2(M_2+M_2^{\times}) + S + S^{\times})\widetilde{H}. \quad (15)
\end{aligned}$$

Together with the following initial conditions

$$\widetilde{H}_1(x, y=0; \boldsymbol{t}=(t_1); \boldsymbol{u}) = u_{(0)}t_1, \quad \widetilde{H}(x, y=0; \boldsymbol{t}; \boldsymbol{u}) = \sum_{i\geq 1} u_{(i)}t_i, \tag{16}$$

determines $\widetilde{H}_1$ *and* $\widetilde{H}$ *uniquely.*

This paper is organized as follows. Section 2 contains basic combinatorial results on the boundary length and point spectra of partial chord diagrams and derives the recursion relation of the number of diagrams (Proposition 2.1), by the cut-and-join method. This cut-and-join equation is rewritten as a second order, non-linear, algebraic partial differential equation for generating function of the number of partial chord diagrams filtered by the boundary length and point spectrum (Proposition 2.2). Section 3 extends these results to include the non-oriented analogues of the partial chord diagrams. The cut-and-join equation is extended to provide a recursion on the number of non-oriented partial chord diagrams (Proposition 3.1), and is also rewritten as partial differential equation (Proposition 3.2).

2. Combinatorial proof of the cut-and-join equation

In this section, we devote to prove Theorem 1.1. The partial differential equation (7) is equivalent to the following recursion relation for the numbers of connected partial chord diagrams.

Proposition 2.1. *The numbers* $\mathcal{M}_{g,k,l}(\boldsymbol{b},\boldsymbol{m})$ *enumerating connected partial chord diagrams of type* $\{g,k,l;\boldsymbol{b},\boldsymbol{m}\}$ *obey the following recursion relation*

$$\begin{aligned}
&k\mathcal{M}_{g,k,l}(\boldsymbol{b},\boldsymbol{m}) \\
&= \sum_{K\geq 1}\sum_{\boldsymbol{d}_K}(m_{\boldsymbol{d}_K}+1)\Bigg[\sum_{1\leq I<J\leq K}\sum_{\ell=0}^{d_I-1}\sum_{m=0}^{d_J-1}\mathcal{M}_{g,k-1,l+2}\left(\boldsymbol{b},\boldsymbol{m}+s_{I,J,\ell,m}(\boldsymbol{d}_K)\right) \\
&\qquad\qquad + \sum_{I=1}^{K}\sum_{\substack{\ell,m=0\\ \ell+m\leq d_I-2}}^{d_I-1}\mathcal{M}_{g,k-1,l+2}\left(\boldsymbol{b},\boldsymbol{m}+s_{I,\ell,m}(\boldsymbol{d}_K)\right)\Bigg] \\
&\quad + \frac{1}{2}\sum_{K\geq 1}\sum_{L\geq 1}\sum_{\boldsymbol{d}_K}\sum_{\boldsymbol{f}_L}(m_{\boldsymbol{d}_K}+1)(m_{\boldsymbol{f}_L}+1-\delta_{\boldsymbol{d}_K,\boldsymbol{f}_L}) \\
&\qquad \times \sum_{I=1}^{K}\sum_{J=1}^{L}\sum_{\ell=0}^{d_I-1}\sum_{m=0}^{f_J-1}\mathcal{M}_{g-1,k-1,l+2}\left(\boldsymbol{b},\boldsymbol{m}+q_{I,J,\ell,m}(\boldsymbol{d}_K,\boldsymbol{f}_L)\right) \\
&\quad + \frac{1}{2}\sum_{K\geq 1}\sum_{L\geq 1}\sum_{\boldsymbol{d}_K}\sum_{\boldsymbol{f}_L}\sum_{g_1+g_2=g}\sum_{k_1+k_2=k-1}\sum_{b^{(1)}+b^{(2)}=b} \\
&\qquad \times \sum_{I=1}^{K}\sum_{J=1}^{L}\sum_{\ell=0}^{d_I-1}\sum_{m=0}^{f_J-1}\sum_{\substack{\boldsymbol{m}^{(1)}+\boldsymbol{m}^{(2)}\\ =\boldsymbol{m}+q_{I,J,\ell,m}(\boldsymbol{d}_K,\boldsymbol{f}_L)}} \\
&\qquad\quad \times m^{(1)}_{\boldsymbol{d}_K}m^{(2)}_{\boldsymbol{f}_L}\frac{b!}{b^{(1)}!b^{(2)}!}\mathcal{M}_{g_1,k_1,l_1}\left(\boldsymbol{b}^{(1)},\boldsymbol{m}^{(1)}\right)\mathcal{M}_{g_2,k_2,l_2}\left(\boldsymbol{b}^{(2)},\boldsymbol{m}^{(2)}\right).
\end{aligned} \tag{17}$$

This recursion relation is referred to as the *cut-and-join equation*, since it follows from a cut-and-join argument, which we shall now provide.

Proof. When one removes one chord from a partial chord diagram, there are essentially three distinct possible outcomes. First of all the diagram can stay connected and then there are two cases to consider. In the first one, the chord that is removed is adjacent to two different boundary components and in the second one it is adjacent to just one. The third case is when the chord diagram becomes disconnected.

In the first case, the genus of the partial chord diagram is not changed, but two boundary components join into one component. On the other hand, in the second case, the genus decreases by one, and one boundary component splits into two components.

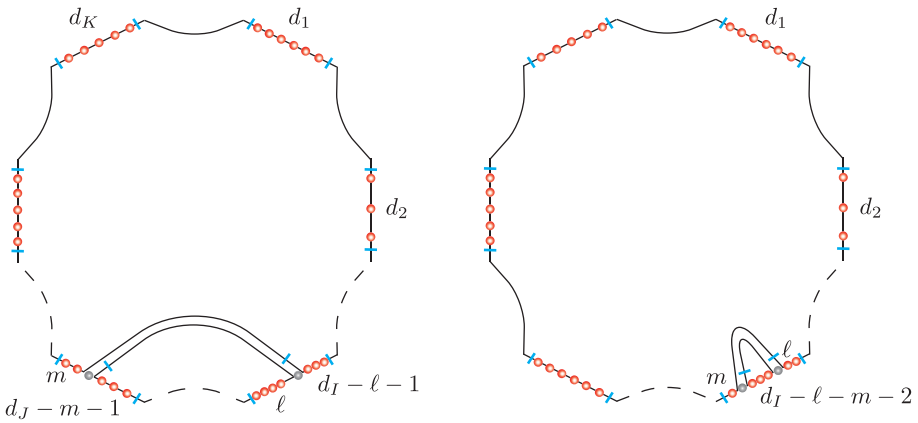

FIGURE 3. Removal of a chord in case one. The chord is depicted as a band. After the removal of this chord, two boundary components join into one component. Left: The clusters of marked points $(d_I-\ell-1, m)$ and (d_J-m-1, ℓ) join into two clusters d_I and d_J Right: The clusters of marked points (ℓ, m) and (d_J-m-1) join into one cluster d_I.

In the first case, and let us say that after removing this chord, the two adjacent boundary components join into one component with the marked point spectrum $\boldsymbol{d}_K = (d_1, \ldots, d_K)$. (See Figure 3.) Under this elimination, the numbers k and n change to $k-1$ and $n-1$, the genus g is not changed (c.f. Euler's relation $2-2g = b-k+n$). The number of marked points l changes to $l+2$, because the chord ends of the chord which is removed become new marked points. There are two distinct possible sub cases, namely either the chord ends belong to two distinct clusters of marked points d_I and d_J in the resulting chord diagram, or chord ends belong to the same cluster of marked points d_I.

We will consider the former kind of chord, and assume $I < J$ without loss of generality. Before we remove the chord, the two boundaries adjacent to the chord needs to have the following two marked point spectra

$$(d_1, \ldots, d_{I-1}, d_I-\ell-1, m, d_{J+1}, \ldots, d_K), \text{ and } (\ell, d_{I+1}, \ldots, d_{J-1}, d_J-m-1),$$
$$0 \leq \ell \leq d_I-1, \quad 0 \leq m \leq d_J-1,$$

When removing the chord, we connect the clusters of marked points $(d_I-\ell-1,m)$ and (d_J-m-1,ℓ). If the original partial chord diagram has the boundary length-point spectrum $\boldsymbol{m}$, the resulting diagram has

$$\begin{aligned}&\boldsymbol{m}-\boldsymbol{e}_{(d_1,\dots,d_{I-1},d_I-\ell-1,m,d_{J+1},\dots,d_K)}-\boldsymbol{e}_{(\ell,d_{I+1},\dots,d_{J-1},d_J-m-1)}+\boldsymbol{e}_{\boldsymbol{d}_K}\\&=\boldsymbol{m}+s_{I,J,\ell,m}(\boldsymbol{d}_K).\end{aligned}$$

For the latter kind, we must have two boundary components with the marked point spectra

$$\begin{aligned}&(d_1,\dots,d_{I-1},\ell,m,d_{I+1},\dots,d_K),\ \text{ and }\ (d_I-\ell-m-2).\\&0\le\ell,m\le d_I-1,\quad 0\le\ell+m\le d_I-2,\end{aligned}$$

and removing the chord connects the clusters of marked points (ℓ,m) and (d_J-m-1). This manipulation changes the boundary length and point spectrum $\boldsymbol{m}$ into

$$\boldsymbol{m}-\boldsymbol{e}_{(d_1,\dots,d_{I-1},\ell,m,d_{I+1},\dots,d_K)}-\boldsymbol{e}_{(d_I-\ell-m-2)}+\boldsymbol{e}_{\boldsymbol{d}_K}=\boldsymbol{m}+s_{I,\ell,m}(\boldsymbol{d}_K).$$

For both of these two kinds of removal, there are $m_{\boldsymbol{d}_K}+1$ possibilities to choose the boundary components in the partial chord diagram. Therefore, the number of possibilities for the first way of removal is

$$\begin{aligned}\sum_{K\ge1}\sum_{\boldsymbol{d}_K}(m_{\boldsymbol{d}_K}+1)\Bigg[&\sum_{1\le I<J\le K}\sum_{\ell=0}^{d_I-1}\sum_{m=0}^{d_J-1}\mathcal{M}_{g,k-1,l+2}\left(\boldsymbol{b},\boldsymbol{m}+s_{I,J,\ell,m}(\boldsymbol{d}_K)\right)\\&+\sum_{I=1}^{K}\sum_{\substack{\ell,m=0\\ \ell+m\le d_I-2}}^{d_I-1}\mathcal{M}_{g,k-1,l+2}\left(\boldsymbol{b},\boldsymbol{m}+s_{I,\ell,m}(\boldsymbol{d}_K)\right)\Bigg].\end{aligned}\tag{18}$$

In the second case (see Figure 4), the removal changes the numbers k and n to $k-1$ and $n+1$ and the genus of the partial chord diagram decreases by one. For partial chord diagram with a boundary with marked point spectrum

$$\begin{aligned}&(d_1,\dots,d_{I-1},d_I-\ell-1,m,f_{J+1},\dots,f_L,f_1,\dots,f_{J-1},f_J-m-1,\ell,d_{I+1},\dots,d_K),\\&0\le\ell\le d_I-1,\quad 0\le m\le f_J-1,\end{aligned}$$

we remove the chord which connects the two clusters (f_J-m-1,ℓ) and $(d_I-\ell-1,m)$ of marked points. The boundary component then splits into two boundary components with marked point spectra $\boldsymbol{d}_K=(d_1,\dots,d_K)$ and $\boldsymbol{f}_L=(f_1,\dots,f_L)$. If the original partial chord diagram has the boundary length and point spectrum $\boldsymbol{m}$, after removal of this chord, we find that

$$\begin{aligned}&\boldsymbol{m}-\boldsymbol{e}_{(d_1,\dots,d_{I-1},d_I-\ell-1,m,f_{J+1},\dots,f_L,f_1,\dots,f_{J-1},f_J-m-1,\ell,d_{I+1},\dots,d_K)}+\boldsymbol{e}_{\boldsymbol{d}_K}+\boldsymbol{e}_{\boldsymbol{f}_L}\\&=\boldsymbol{m}+q_{I,J,\ell,m}(\boldsymbol{d}_K,\boldsymbol{f}_L).\end{aligned}$$

The number of possibilities of this removal is $(m_{\boldsymbol{d}_K}+1)(m_{\boldsymbol{f}_L}+1)$ for $\boldsymbol{d}_K\neq\boldsymbol{f}_L$. If $\boldsymbol{d}_K=\boldsymbol{f}_L$, the number of possibilities becomes $m_{\boldsymbol{d}_K}(m_{\boldsymbol{d}_K}+1)/2$. In total, the

number of possibilities for the second way of elimination is

$$\frac{1}{2}\sum_{K=1}^{\infty}\sum_{L=1}^{\infty}\sum_{\boldsymbol{d}_K}\sum_{\boldsymbol{f}_L}(m_{\boldsymbol{d}_K}+1)(m_{\boldsymbol{f}_L}+1-\delta_{\boldsymbol{d}_K,\boldsymbol{f}_L}) \times\sum_{I=1}^{K}\sum_{J=1}^{L}\sum_{\ell=0}^{d_I-1}\sum_{h=0}^{f_J-1}\mathcal{M}_{g-1,k-1,l+2}\left(\boldsymbol{b},\boldsymbol{m}+q_{I,J,\ell,h}(\boldsymbol{d}_K,\boldsymbol{f}_L)\right). \tag{19}$$

The factor $1/2$ in front of the sum takes care of the over counting in the cases $\boldsymbol{d}_K \neq \boldsymbol{f}_L$.

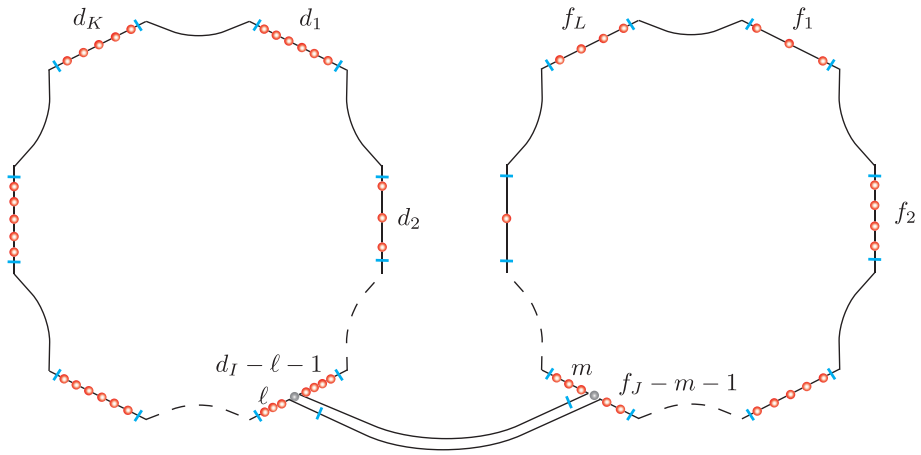

FIGURE 4. The second and third way of elimination of a chord. After the elimination of this chord, a boundary component split into two different boundary components.

In the third case, the partial chord diagram split into two connected components. We consider the case that the original diagram has the type $\{g,k,l;\boldsymbol{b},\boldsymbol{m}\}$ and the resulting two connected components have types $\{g_1,k_1,l_1;\boldsymbol{b}^{(1)},\boldsymbol{m}^{(1)}\}$ and $\{g_2,k_2,l_2;\boldsymbol{b}^{(2)},\boldsymbol{m}^{(2)}\}$. These types are related such that

$$g=g_1+g_2,\quad k-1=k_1+k_2,\quad \boldsymbol{b}=\boldsymbol{b}^{(1)}+\boldsymbol{b}^{(2)}.$$

Since a boundary component also split into two components, the boundary length and point spectrum changes in the same manner as in the second case.

$$\boldsymbol{m}+q_{I,J,\ell,m}(\boldsymbol{d}_K,\boldsymbol{f}_L)=\boldsymbol{m}^{(1)}+\boldsymbol{m}^{(2)}.$$

There are $m^{(1)}_{\boldsymbol{d}_K}m^{(2)}_{\boldsymbol{f}_L}$ ways to choose the boundary components which are to be fused under the inverse operation of chord removal. And the number of different ordered splittings of a b-backbone diagram is $\frac{b!}{b^{(1)}!b^{(2)}!}$ where $b^{(a)}=\sum_i b_i^{(a)}$ $(a=$

$1,2$). Therefore, the total number of possibilities of this case is

$$\frac{1}{2}\sum_{I=1}^{\infty}\sum_{J=1}^{\infty}\sum_{\boldsymbol{d}_K}\sum_{\boldsymbol{f}_L}\sum_{g_1+g_2=g}\sum_{k_1+k_2=k-1}\sum_{b^{(1)}+b^{(2)}=b}$$
$$\times\sum_{I=1}^{K}\sum_{J=1}^{L}\sum_{\ell=0}^{d_I-1}\sum_{m=0}^{f_J-1}\sum_{\substack{\boldsymbol{m}^{(1)}+\boldsymbol{m}^{(2)}\\=\boldsymbol{m}+q_{I,J,\ell,m}(\boldsymbol{d}_K,\boldsymbol{f}_L)}}$$
$$\times m^{(1)}_{\boldsymbol{d}_K}m^{(2)}_{\boldsymbol{f}_L}\frac{b!}{b^{(1)}!b^{(2)}!}\mathcal{M}_{g_1,k_1,l_1}\big(\boldsymbol{b}^{(1)},\boldsymbol{m}^{(1)}\big)\mathcal{M}_{g_2,k_2,l_2}\big(\boldsymbol{b}^{(2)},\boldsymbol{m}^{(2)}\big). \tag{20}$$

The factor $1/2$ corrects for the over counting due to the ordering of the two connected components.

The sum of the contributions (18), (19), and (20) from the three different cases of chord removals equals $k\mathcal{M}_{g,k,l}(\boldsymbol{b},\boldsymbol{m})$, because there are k possibilities for the choice of the chord to be removed. This gives the cut-and-join equation (17). □

Proposition 2.2. *The generating function $H(x,y;\boldsymbol{t},;\boldsymbol{u})$ is uniquely determined by the differential equation*

$$\frac{\partial H}{\partial y}=(M+S)H,$$

where $M=M_0+x^2M_2$. The generating function $Z(x,y;\boldsymbol{t},;\boldsymbol{u})=\exp[H]$ of the number of connected and disconnected partial chord diagrams satisfies

$$\frac{\partial Z}{\partial y}=MZ, \tag{21}$$

and is as such determined by the initial conditions

$$H(x,y=0;\boldsymbol{t};\boldsymbol{u})=\sum_{i\geq 1}t_iu_{(i)},\quad Z(x,y=0;\boldsymbol{t},;\boldsymbol{u})=\mathrm{e}^{\sum_{i\geq 1}t_iu_{(i)}}.$$

Proof. It is straightforward to check that the differential equation $\frac{\partial H}{\partial y}=(M+S)H$ is equivalent to the cut-and-join equation (17). The actions in the quadratic differential S on H can be rewritten by following relation

$$D_{\boldsymbol{d}_K}(H)D_{\boldsymbol{f}_L}(H)+D_{\boldsymbol{d}_K}D_{\boldsymbol{f}_L}H=\frac{1}{Z}D_{\boldsymbol{d}_K}D_{\boldsymbol{f}_L}Z.$$

The derivatives on the right hand side are contained in M_2, and the differential equation $\frac{\partial Z}{\partial y}=MZ$ follows from that of H.

On the initial condition, every partial chord diagram of type $\{g,k,l;\boldsymbol{b};\boldsymbol{m}\}$ can be obtained from the disjoint collection of type $\{0,0,i;\boldsymbol{e}_i,\boldsymbol{e}_{(i)}\}$ with multiplicity b_i by connecting them with k chords. This implies $H(x,y=0;\boldsymbol{t};\boldsymbol{u})=\sum_{i\geq 1}t_iu_{(i)}$. Since this is the first order differential equation of y, the coefficient of y^k is determined uniquely using this initial condition.

□

3. Non-oriented analogue of the cut-and-join equation

In this section, we will prove Theorem 1.2. We first establish the following proposition.

Proposition 3.1. *The number $\widetilde{\mathcal{M}}_{g,k,l}(\boldsymbol{b},\boldsymbol{m})$ of connected non-oriented partial chord diagrams of type $\{g,k,l;\boldsymbol{b},\boldsymbol{m}\}$ obeys the following recursion relation*

$$
\begin{aligned}
&k\widetilde{\mathcal{M}}_{g,k,l}(\boldsymbol{b},\boldsymbol{m})\\
&=\sum_{K\geq 1}\sum_{\boldsymbol{d}_K}(m_{\boldsymbol{d}_K}+1)\\
&\quad\times\Bigg[\sum_{I<J}\sum_{\ell=0}^{d_I-1}\sum_{m=0}^{d_J-1}\Big\{\widetilde{\mathcal{M}}_{h,k-1,l+2}\left(\boldsymbol{b},\boldsymbol{m}+s_{I,J,\ell,m}(\boldsymbol{m})\right)+\widetilde{\mathcal{M}}_{h-1,k-1,l+2}\big(\boldsymbol{b},\boldsymbol{m}+s^{\times}_{I,J,\ell,m}(\boldsymbol{m})\big)\Big\}\\
&\quad+\sum_{I=1}^{K}\sum_{\ell+m\leq d_I-2}\Big\{\widetilde{\mathcal{M}}_{h,k-1,l+2}\left(\boldsymbol{b},\boldsymbol{m}+s_{I,\ell,m}(\boldsymbol{m})\right)+\widetilde{\mathcal{M}}_{h-1,k-1,l+2}\big(\boldsymbol{b},\boldsymbol{m}+s^{\times}_{I,\ell,m}(\boldsymbol{m})\big)\Big\}\Bigg]\\
&\quad+\frac{1}{2}\sum_{K\geq 1}\sum_{L\geq 1}\sum_{\boldsymbol{d}_K}\sum_{\boldsymbol{f}_L}(m_{\boldsymbol{d}_K}+1)(m_{\boldsymbol{f}_L}+1-\delta_{\boldsymbol{d}_K,\boldsymbol{f}_L})\\
&\quad\times\sum_{I=1}^{K}\sum_{J=1}^{L}\sum_{\ell=0}^{d_I-1}\sum_{m=0}^{f_J-1}\Big\{\widetilde{\mathcal{M}}_{h-2,k-1,l+2}\left(\boldsymbol{b},\boldsymbol{m}+q_{I,J,\ell,m}(\boldsymbol{d}_K,\boldsymbol{f}_L)\right)\\
&\qquad\qquad+\widetilde{\mathcal{M}}_{h-2,k-1,l+2}\big(\boldsymbol{b},\boldsymbol{m}+q^{\times}_{I,J,\ell,m}(\boldsymbol{d}_K,\boldsymbol{f}_L)\big)\Big\}\\
&\quad+\frac{1}{2}\sum_{K\geq 1}\sum_{L\geq 1}\sum_{\boldsymbol{d}_K}\sum_{\boldsymbol{f}_L}\sum_{h_1+h_2=h}\sum_{k_1+k_2=k-1}\sum_{b^{(1)}+b^{(2)}=b}\\
&\quad\times\sum_{I=1}^{K}\sum_{J=1}^{L}\sum_{\ell=0}^{d_I-1}\sum_{m=0}^{f_J-1}\left(\sum_{\substack{\boldsymbol{m}^{(1)}+\boldsymbol{m}^{(2)}\\=\boldsymbol{m}+q_{I,J,\ell,m}(\boldsymbol{d}_K,\boldsymbol{f}_L)}}+\sum_{\substack{\boldsymbol{m}^{(1)}+\boldsymbol{m}^{(2)}\\=\boldsymbol{m}+q^{\times}_{I,J,\ell,m}(\boldsymbol{d}_K,\boldsymbol{f}_L)}}\right)m^{(1)}_{\boldsymbol{d}_K}m^{(2)}_{\boldsymbol{f}_L}\\
&\quad\times\frac{b!}{b^{(1)}!b^{(2)}!}\widetilde{\mathcal{M}}_{h_1,k_1,l_1}\big(\boldsymbol{b}^{(1)},\boldsymbol{m}^{(1)}\big)\widetilde{\mathcal{M}}_{h_2,k_2,l_2}\big(\boldsymbol{b}^{(2)},\boldsymbol{m}^{(2)}\big).
\end{aligned}
\tag{22}
$$

Proof. If we remove a non-twisted chord, then we find the same recursive structure as for the numbers (18), (19), and (20) for $\widetilde{\mathcal{M}}_{h,k,l}\big(\boldsymbol{b},\boldsymbol{m}\big)$ in the oriented case. As we did in the proof of proposition 2.1, we also consider three cases, organised the same way, when removing a twisted chord.

In the first case (see Figure 5), there are again two possibilities, namely the twisted chord ends belong to two different or the same clusters of marked points on the boundary component in the resulting diagram after removal. Contrary to the case of non-twisted chords, the boundary cycle does not split, but the marked point spectrum changes due to the recombination of the boundary component. For both of these two cases, the numbers k and n change to $k-1$ and n, and the cross-cap number h decreases by one under this elimination (c.f. Euler's relation $2-h=b-k+n$). The chord ends become marked points and l changes to $l+2$.

In the former situation, we must have a boundary component with the marked point spectrum

$$
\begin{aligned}
&(d_1,\ldots,d_{I-1},\ell,m,d_{J-1},d_{J-2}\ldots,d_{I+1},d_I-\ell-1,d_J-m-1,d_{J+1},\ldots,d_K)\\
&I<J,\quad 0\leq\ell\leq d_I-1,\quad 0\leq m\leq d_J-1,
\end{aligned}
$$

from which we remove one twisted chord with one end between the two clusters (ℓ,m) and the other between $(d_I-\ell-1,d_J-m-1)$. Then the removal will result

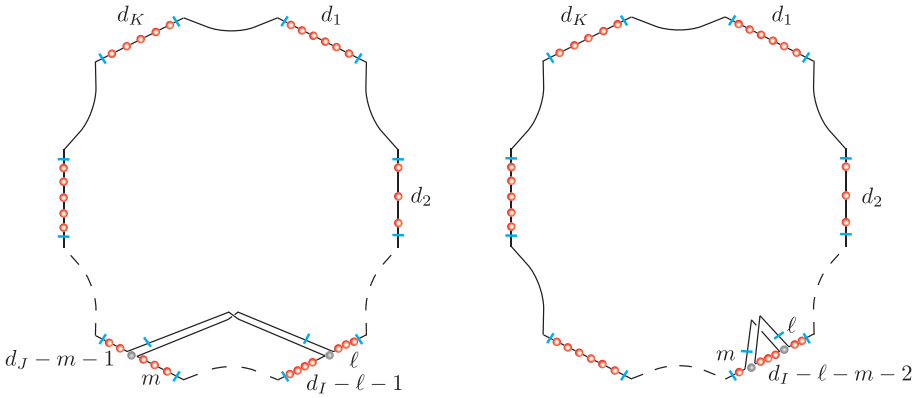

FIGURE 5. Removal of a twisted chord from a non-oriented partial chord diagram. The chord is depicted as a twisted band. After the elimination of this chord, the boundary component is reconnected into one component with different marked point spectrum. Left: The clusters of marked points $(d_I - \ell - 1, m)$ and $(d_J - m - 1, \ell)$ join into two clusters d_I and d_J. Right: The clusters of marked points (ℓ, m) and $(d_J - m - 1)$ join into one cluster d_I.

in a boundary component with the marked point spectrum $\boldsymbol{d}_K$ and the boundary length and point spectrum $\boldsymbol{m}$ is changed as follows

$$\begin{aligned}&\boldsymbol{m} - \boldsymbol{e}_{(d_1,\dots,d_{I-1},\ell,m,d_{J-1},\dots,d_{J+1},d_J-\ell-1,d_J-m-1,d_{J+1},\dots,d_K)} + \boldsymbol{e}_{\boldsymbol{d}_K}\\ &= \boldsymbol{m} + s^{\times}_{I,J,\ell,m}(\boldsymbol{d}_K).\end{aligned}$$

The possible number of choices for this kind of removal is $m_{\boldsymbol{d}_K} + 1$, and the total number of diagrams which can be obtained in this way is

$$\sum_{K\geq 1}\sum_{\boldsymbol{d}_K}(m_{\boldsymbol{d}_K}+1)\sum_{I<J}\sum_{\ell=0}^{d_I-1}\sum_{m=0}^{d_J-1}\widetilde{\mathcal{M}}_{h-1,k-1,l+2}\big(\boldsymbol{b},\boldsymbol{m}+s^{\times}_{I,J,\ell,m}(\boldsymbol{m})\big). \tag{23}$$

For the removal of the latter kind of twisted chords, we must start with a diagram with a boundary component with the marked point spectrum

$$\begin{aligned}&(d_1,\dots,d_{I-1},\ell,d_I-\ell-m-2,m,d_{I+1},\dots,d_K),\\ &0\leq \ell,m\leq d_I,\quad \ell+m\leq d_I-2.\end{aligned}$$

from which we remove one twisted chords with one end between the two clusters $(\ell, d_I - \ell - m - 2)$ and the other one between the two clusters $(d_I - \ell - m - 2, m)$. After removal, we obtain a boundary component with the marked point spectrum $\boldsymbol{d}_K$. Thus, the boundary length and point spectrum $\boldsymbol{m}$ is changed to

$$\boldsymbol{m} - \boldsymbol{e}_{(d_1,\dots,d_{I-1},\ell,d_I-\ell-m-2,m,d_{I+1},\dots,d_K)} + \boldsymbol{e}_{\boldsymbol{d}_K} = \boldsymbol{m} + s^{\times}_{I,\ell,m}(\boldsymbol{d}_K).$$

The number of such chords to be removed is $m_{\boldsymbol{d}_K} + 1$, and the total number of partial chord diagrams obtained in this way is

$$\sum_{K\geq 1}\sum_{\boldsymbol{d}_K}(m_{\boldsymbol{d}_K}+1)\sum_{I=1}^{K}\sum_{\ell+m\leq d_I-2}\widetilde{\mathcal{M}}_{h-1,k-1,l+2}\big(\boldsymbol{b},\boldsymbol{m}+s^{\times}_{I,\ell,m}(\boldsymbol{m})\big). \tag{24}$$

Next, we consider the second case (see Figure 6), where we must start with a non-oriented partial chord diagram with a boundary component with the marked point spectrum

$$(f_1,\dots,f_{J-1},f_J-m-1,\ell,d_{I-1},\dots,d_1,d_K,\dots,d_{I+1},d_I-\ell-1,m,f_{J+1},\dots,f_L),$$
$$0\leq \ell\leq d_I-1,\quad 0\leq m\leq f_J-1,$$

from which we remove a twisted chord with one end between the two clusters (f_J-m-1,ℓ) and the other end between the two clusters $(d_I-\ell-1,m)$. After removal of this chord, the boundary component has been split into two components with spectra $\boldsymbol{d}_K$ and $\boldsymbol{f}_L$, and the cross-cap number h decreases by two. Then, the boundary length and point spectrum $\boldsymbol{m}$ changes to

$$\begin{aligned}&\boldsymbol{m}-\boldsymbol{e}_{(f_1,\dots,f_{J-1},f_J-m-1,\ell,d_{I-1},\dots,d_1,d_K,\dots,d_{I+1},d_I-\ell-1,m,f_{J+1},\dots,f_L)}+\boldsymbol{e}_{\boldsymbol{d}_K}+\boldsymbol{e}_{\boldsymbol{f}_L}\\&=\boldsymbol{m}+q^{\times}_{I,J,\ell,m}(\boldsymbol{d}_K,\boldsymbol{f}_L).\end{aligned}$$

The number of choices for the chord to be removed is $(m_{\boldsymbol{d}_K}+1)(m_{\boldsymbol{f}_L}+1)$ for $\boldsymbol{d}_K\neq\boldsymbol{f}_L$ and $m_{\boldsymbol{d}_K}(m_{\boldsymbol{d}_K}+1)/2$ for $\boldsymbol{d}_K=\boldsymbol{f}_L$, and the total number of partial chord diagrams obtained this way is

$$\begin{aligned}&\frac{1}{2}\sum_{K\geq 1}\sum_{L\geq 1}\sum_{\boldsymbol{d}_K}\sum_{\boldsymbol{f}_L}(m_{\boldsymbol{d}_K}+1)(m_{\boldsymbol{f}_L}+1-\delta_{\boldsymbol{d}_K,\boldsymbol{f}_L})\\&\times\sum_{I=1}^{K}\sum_{J=1}^{L}\sum_{\ell=0}^{d_I-1}\sum_{m=0}^{f_J-1}\widetilde{\mathcal{M}}_{h-2,k-1,l+2}\big(\boldsymbol{b},\boldsymbol{m}+q^{\times}_{I,J,\ell,m}(\boldsymbol{d}_K,\boldsymbol{f}_L)\big).\end{aligned}\tag{25}$$

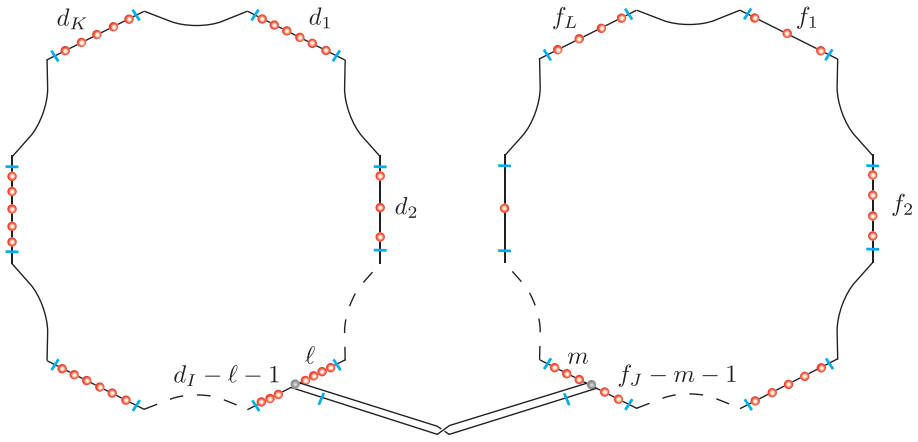

FIGURE 6. The second case of a twisted chord removal. After the removal of this chord, the boundary component split into two distinct boundary components.

In case three partial chord diagram split into two connected components when we remove the chord. Assume that the original diagram has the type $\{h,k,l;\boldsymbol{b},\boldsymbol{m}\}$ and the resulting two connected components have types $\{h_1,k_1,l_1;\boldsymbol{b}^{(1)},\boldsymbol{m}^{(1)}\}$ and $\{h_2,k_2,l_2;\boldsymbol{b}^{(2)},\boldsymbol{m}^{(2)}\}$. Then these types are related by

$$h=h_1+h_2,\quad k-1=k_1+k_2,\quad \boldsymbol{b}=\boldsymbol{b}^{(1)}+\boldsymbol{b}^{(2)}.$$

The marked point spectrum changes in the same way as the second case

$$\boldsymbol{m} + q^{\times}_{I,J,\ell,m}(\boldsymbol{d}_K, \boldsymbol{f}_L) = \boldsymbol{m}^{(1)} + \boldsymbol{m}^{(2)}.$$

The total number of resulting diagrams is

$$\begin{aligned}
&\frac{1}{2}\sum_{K\geq 1}\sum_{L\geq 1}\sum_{\boldsymbol{d}_K}\sum_{\boldsymbol{f}_L}\sum_{h_1+h_2=h}\sum_{k_1+k_2=k-1}\sum_{b^{(1)}+b^{(2)}=b}\\
&\quad\times\sum_{I=1}^{K}\sum_{J=1}^{L}\sum_{\ell=0}^{d_I-1}\sum_{m=0}^{f_J-1}\sum_{\substack{\boldsymbol{m}^{(1)}+\boldsymbol{m}^{(2)}\\ =\boldsymbol{m}+q^{\times}_{I,J,\ell,m}(\boldsymbol{d}_K,\boldsymbol{f}_L)}}\\
&\quad\times m^{(1)}_{\boldsymbol{d}_K} m^{(2)}_{\boldsymbol{f}_L}\frac{b!}{b^{(1)}!b^{(2)}!}\widetilde{\mathcal{M}}_{h_1,k_1,l_1}\big(\boldsymbol{b}^{(1)},\boldsymbol{m}^{(1)}\big)\widetilde{\mathcal{M}}_{h_2,k_2,l_2}\big(\boldsymbol{b}^{(2)},\boldsymbol{m}^{(2)}\big). \qquad (26)
\end{aligned}$$

Therefore, in total, the number of possible partial chord diagrams obtained by removing a twisted or a non-twisted chord is the sum of (23) – (26) and of (18) – (20) for $\widetilde{\mathcal{M}}_{h,k,l}\big(\boldsymbol{b},\boldsymbol{m}\big)$. This number gives the right hand side of equation (22), which we have just argued also gives the left side of equation (22).

□

Along the same line of arguments as the ones which proved Proposition 2.2, we obtain the proposition below.

Proposition 3.2. *The generating function $\widetilde{H}(x,y;\boldsymbol{t},;\boldsymbol{u})$ is uniquely determined by the differential equation*

$$\frac{\partial\widetilde{H}}{\partial y} = (\widetilde{M} + \widetilde{S})\widetilde{H},$$

where $\widetilde{M} = M_0 + xM_1^{\times} + x^2(M_2 + M_2^{\times})$ and $\widetilde{S} = S + S^{\times}$. The generating function $\widetilde{Z}(x,y;\boldsymbol{t},;\boldsymbol{u}) = \exp[\widetilde{H}]$ of the number of connected and disconnected partial chord diagrams filtered by the boundary length and point spectrum satisfies

$$\frac{\partial\widetilde{Z}}{\partial y} = \widetilde{M}\widetilde{Z}. \qquad (27)$$

As such they are uniquely determined by the initial conditions

$$\widetilde{H}(x,y=0;\boldsymbol{t};\boldsymbol{u}) = \sum_{i\geq 1} t_i u_{(i)}, \quad \widetilde{Z}(x,y=0;\boldsymbol{t},;\boldsymbol{u}) = \mathrm{e}^{\sum_{i\geq 1} t_i u_{(i)}}.$$

References

[1] N. V. Alexeev, J. E. Andersen, R. C. Penner, and P. Zograf, *Enumeration of Chord Diagrams on many intervals and their non-orientable analogs,* Adv. Math. **289** (2016) 1056–1081, arXiv:1307.0967 [math.CO].

[2] J. E. Andersen, A. J. Bene, J. -B. Meilhan, and R. C. Penner, *Finite type invariants and fatgraphs,* Adv. Math. **225** (2010), 2117–2161.

[3] J. E. Andersen, L. O. Chekhov, R. C. Penner, C. M. Reidys, and P. Sulkowski, *Topological recursion for chord diagrams, RNA complexes, and cells in moduli spaces,* Nucl. Phys. **B866** (2013) 414-443, arXiv:1205.0658 [hep-th].

[4] J. E. Andersen, L. O. Chekhov, R. C. Penner, C. M. Reidys, and P. Sulkowski, *Enumeration of RNA complexes via random matrix theory,* Biochem. Soc. Trans. **41** (2013) 652-655, arXiv:1303.1326 [q-bio.QM].

[5] J. E. Andersen, H. Fuji, M. Manabe, R. C. Penner, P. Sulkowski, *Enumeration of chord diagrams via topological recursion and quantum curve techniques*, Preprint.

[6] J. E. Andersen, H. Fuji, M. Manabe, R. C. Penner, P. Sulkowski, *Partial chord diagrams and matrix models*, Preprint.
[7] J. E. Andersen, F. W. D. Huang, R. C. Penner, C. M. Reidys, *Topology of RNA-RNA interaction structures,* J. Comp. Biol. **19** (2012) 928-943, arXiv:1112.6194 [math.CO].
[8] J. E. Andersen, J. Mattes, and N. Reshetikhin, *The Poisson Structure on the Moduli Space of Flat Connections and Chord Diagrams,* Topology **35** (1996) 1069–1083.
[9] J. E. Andersen, J. Mattes, and N. Reshetikhin, *Quantization of the algebra of chord diagrams,* Math. Proc. Camb. Phil. Soc. **124** (1998) 451–467.
[10] J. E. Andersen, R. C. Penner, C. M. Reidys, R. R. Wang, *Linear chord diagrams on two intervals,* arXiv:1010.5857 [math.CO].
[11] J. E. Andersen, R. C. Penner, C. M. Reidys, M. S. Waterman, *Enumeration of linear chord diagrams,* J. Math. Biol. **67** (2013) 1261–78, arXiv:1010.5614 [math.CO].
[12] D. Bar-Natan, *On the Vassiliev knot invariants,* Topology **34** (1995) 423–475.
[13] R. Campoamor-Stursberg and V. O. Manturov, *Invariant tensor formulas via chord diagrams,* Jour. Math. Sci. **108** (2004) 3018–3029.
[14] J. Courtiel, K. Yeats, *Terminal chords in connected chord diagrams,* arXiv:1603.08596 [math.CO].
[15] M. Kontsevich, *Vassilievs knot invariants,* Adv. Sov. Math. **16** (1993) 137–150.
[16] N. Marie, and K. Yeats, *A chord diagram expansion coming from some Dyson-Schwinger equations,* Comm. Numb. Theo. Phys. **7** (2013) 251–291, arXiv:1210.5457 [math.CO].
[17] H. Orland, and A. Zee, *RNA Folding and Large N Matrix Theory,* Nucl. Phys. **B620** (2002) 456-476, arXiv:cond-mat/0106359 [cond-mat.stat-mech].
[18] R. C. Penner, *The decorated Teichmüller space of punctured surfaces,* Comm. Math. Phys. **113** (1987) 299–339.
[19] R. C. Penner, *Perturbative series and the moduli space of Riemann surfaces,* J. Diff. Geom. **27** (1988) 35–53.
[20] R. C. Penner, *The simplicial compactification of Riemann's moduli space,* Proceedings of the 37th Taniguchi Symposium, World Scientific (1996), 237–252.
[21] R. C. Penner, *Cell decomposition and compactification of Riemann's moduli space in decorated Teichmüller theory,* In Tongring, N. and Penner, R.C. (eds) Woods Hole Mathematics-Perspectives in Math and Physics, World Scientific, Singapore, arXiv:math/0306190 [math.GT].
[22] R. C. Penner, *Moduli spaces and macromolecules,* Bull. Amer. Math. Soc. (2016).
[23] C. M. Reidys, *Combinatorial and computational biology of pseudoknot RNA,* Springer, Applied Math series 2010.
[24] G. Vernizzi, and H. Orland, *Large-N Random Matrices for RNA Folding,* Acta Phys. Polon. **B36** (2005) 2821-2827.
[25] G. Vernizzi, H. Orland, and A. Zee, *Enumeration of RNA structures by Matrix Models,* Phys. Rev. Lett. **94** 168103, arXiv:q-bio/0411004 [q-bio.BM].

QGM, Department of Mathematics, Aarhus University, DK-8000 Aarhus C, Denmark
E-mail address: jea.qgm@gmail.com

Faculty of Education, Kagawa University, Takamatsu 760-8522, Japan
E-mail address: fuji@ed.kagawa-u.ac.jp

Institut des Hautes Études Scientifiques, 35 route de Chartres, 91440 Burs-sur-Yvette, France; Division of Physics, Mathematics and Astronomy, California Institute of Technology, Pasadena, CA 91125, USA
E-mail address: rpenner@caltech.edu, rpenner@ihes.fr

Biocomplexity Institute of Virginia Tech Blacksburg, VA 24061, USA
E-mail address: duckcr@vbi.vt.edu